Formal Definition of the ODE of RNAi and Experimental Results for Approximate Abstraction

Ibuki Kawamata

Graduate School of Information Science and Technology, University of Tokyo
7-3-1 Hongo, Bunkyo-ku, Tokyo, 113-8656, Japan
ibuki@is.s.u-tokyo.ac.jp

1 Introduction

This document is a supplementary document of the paper "Abstraction of Graph-Based Models of Bio-Molecular Reaction Systems for Efficient Simulation" that is submitted to CMSB2012. I recommend to read the article in advance.

In this document, I give formal definitions of the ODE for RNAi. I also give detail experimental results to understand an approximate abstraction of RNAi simulation.

2 Naive model

In the naive model of RNAi 1, we allocated variable to each global structure. The number of segments n that is cleaved by DICER is the main parameter for this model.

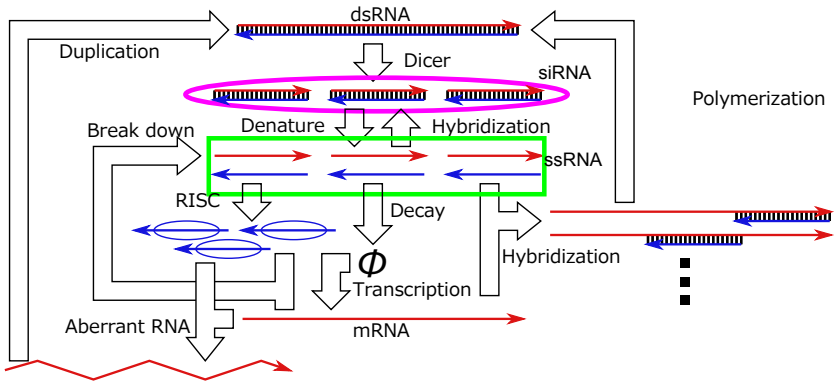

Fig. 1. Schematic explanation of RNAi

We allocate variables

$$
\begin{aligned}
&[dsRNA] \\
&[siRNA_1], \cdots, [siRNA_n] \\
&[ssRNA_1^u], \cdots, [ssRNA_n^u] \\
&[ssRNA_1^l], \cdots, [ssRNA_n^l]
\end{aligned}
$$

to global structures in the center column of the figure. For the concentration fo mRNA, we allocate variables $[mRNA]$, which is constantly produces by transcription reaction. Differential equations for each reaction is defined as follows. Note that differential equations for each variable are sum up to construct the whole differential equations. Dicer:

$$
\begin{aligned}
\frac{d[dsRNA]}{dt} &= -k_{dicer}[dsRNA] \\
\frac{d[siRNA_i]}{dt} &= k_{dicer}[dsRNA] \ \ (i \in \{1, \cdots n\})
\end{aligned}
$$

Denature:

$$
\begin{aligned}
\frac{d[siRNA_i]}{dt} &= -k_{denature}[siRNA_i] \ (i \in \{1, \cdots n\}) \\
\frac{d[ssRNA_i^u]}{dt} &= k_{denature}[siRNA_i] \ \ (i \in \{1, \cdots n\}) \\
\frac{d[ssRNA_i^l]}{dt} &= k_{denature}[siRNA_i] \ \ (i \in \{1, \cdots n\})
\end{aligned}
$$

Hybridization:

$$
\begin{aligned}
\frac{d[siRNA_i]}{dt} &= k_{hybridization}[ssRNA_i^u][ssRNA_i^l] \ (i \in \{1, \cdots n\}) \\
\frac{d[ssRNA_i^u]}{dt} &= k_{hybridization}[ssRNA_i^u][ssRNA_i^l] \ (i \in \{1, \cdots n\}) \\
\frac{d[ssRNA_i^l]}{dt} &= k_{hybridization}[ssRNA_i^u][ssRNA_i^l] \ (i \in \{1, \cdots n\})
\end{aligned}
$$

Decay:

$$
\begin{aligned}
\frac{d[ssRNA_i^u]}{dt} &= -k_{decay}[ssRNA_i^u] \ (i \in \{1, \cdots n\}) \\
\frac{d[ssRNA_i^l]}{dt} &= k_{decay}[ssRNA_i^l] \ \ \ (i \in \{1, \cdots n\}) \\
\frac{d[mRNA]}{dt} &= k_{decay}[mRNA]
\end{aligned}
$$

Transcription:

$$
\frac{d[mRNA]}{dt} = k_{transcription}
$$

Hybridization reactions between siRNA and mRNA produce combinatorial number of partially double-helical structures. Because it is difficult to list all the variables for partially double-helical structures, I explain how to construct new structures by reaction rules. Reaction rules for partially double-helical structures are, Hybridization, Denature, and Polymerization.

2.1 Hybridization

Hybridization occur between a partially double-helical structure (including $mRNA$) and one of the $ssRNA_i^l (i \in \{1, \cdots n\})$ if the complementary part is still accessible.

$$\frac{d[s_i]}{dt} = k_{hybridization}[ssRNA_i^l][s_i] \quad (i \in \{1, \cdots n\}, s^i \in S_i)$$
$$\frac{d[ssRNA_i^l]}{dt} = k_{hybridization}[ssRNA_i^l][s_i] \ (i \in \{1, \cdots n\}, s^i \in S_i)$$

where, S_i denotes a set of partially double-helical structures in which ith position is not hybridized yet and still accessible.

2.2 Denature

Denature is an inverse reaction of hybridization where short (one segment) RNA is separated from partially double-helical structure and become one of the $ssRNA_i^l (i \in \{1, \cdots n\})$.

$$\frac{d[s_i']}{dt} = -k_{denature}[s_i'] \quad (i \in \{1, \cdots n\}, s_i' \in S_i')$$
$$\frac{d[ssRNA_i^l]}{dt} = k_{denature}[s_i'] \ (i \in \{1, \cdots n\}, s_i' \in S_i')$$

where, S_i' denotes a set of partially double-helical structures in which ith position is hybridized by a one-segment RNA.

2.3 Polymerization

Polymerization extends the phosphate backbone of RNA which correspond to extend one segment in the model.

$$\frac{d[s]}{dt} = -k_{polymerization}[s] \ (s \in S)$$
$$\frac{d[s+]}{dt} = k_{polymerization}[s]$$

where S denotes a set of partially double-helical structures in which there is a primer RNA that can be extended and $s+$ correspond to partially double-helical structure that is extended.

3 Local model

By abstracting the original model, we defined a local model that is focused on repeatedly appearing sub-graphs. Local model is also explained as ODEs system. The number of local structures with specific position is limited to 26. Note that only 7 of them are required in the corner.

4 Refined model

By refining the local model, we defined a refined model that tries to reproduce the concentration of dsRNA more accurately. In the refined model, three of local structures are divided into two structures, one of which is a local structure that can construct dsRNA, and the other of which is a local structure that cannot. The number of local structures of specific position becomes 29.

5 Result of abstraction

We also compared the concentration change of dsRNA among the three models (Fig. 2, Fig. 3, Fig. 4). x and y-axes of the graph are time and concentration of dsRNA, respectively. Although the normal local model had a slight difference from the naive model, the refined local model had almost no difference. This result suggests that the refined local model is more exactly calculating the concentration of dsRNA than the normal local model. Note that the naive original model gave exact simulation because all structures were took into account.

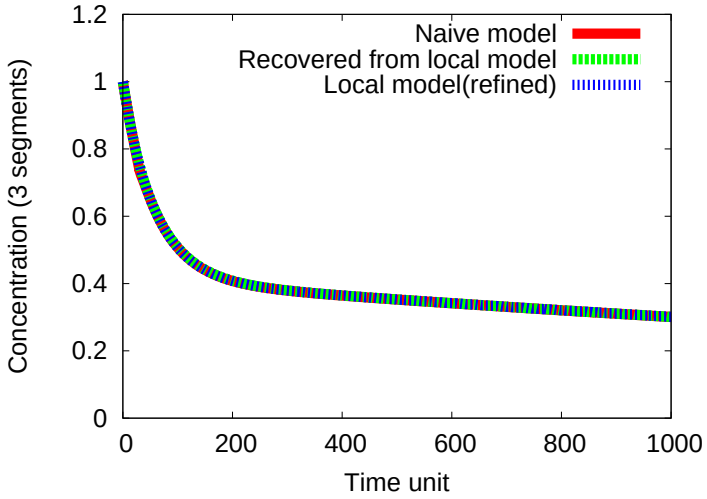

Fig. 2. Concentration ofdsRNA (3 segments)

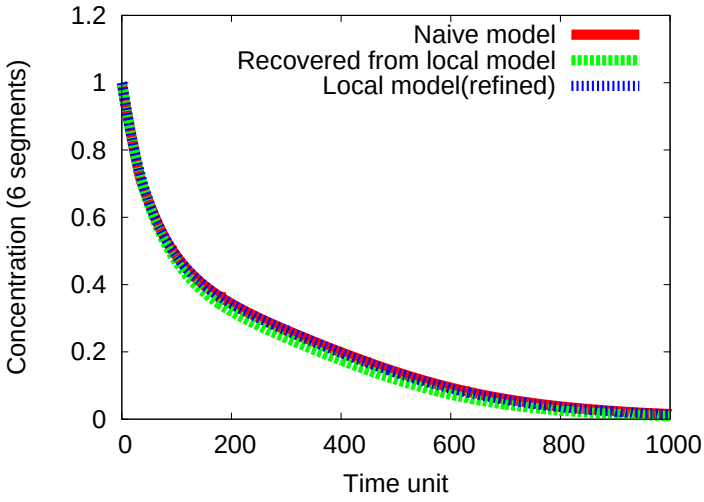

Fig. 3. Concentration ofdsRNA (6 segments)

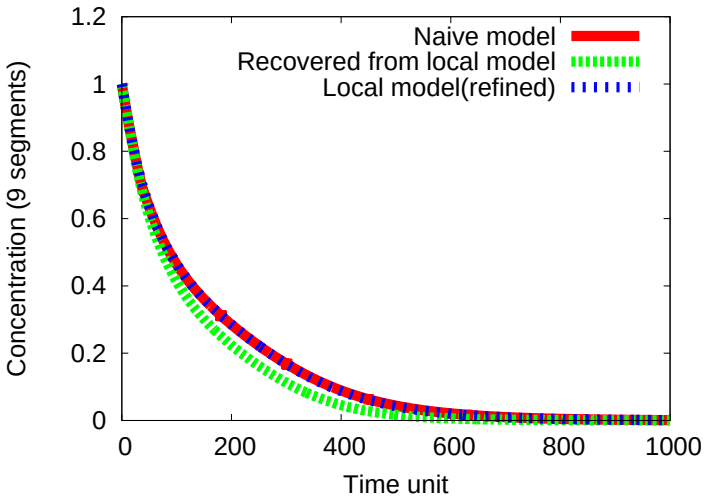

Fig. 4. Concentration ofdsRNA (9 segments)

Though we can empirically conclude that both local models are calculating the concentration of dsRNA accurately, their results are theoretically approximate. This is due to the ratio assumption. By calculating the time change of ratios, we examined the exactness of the ratio assumption for local models. To calculate a ratio, we first select one local structure and find all the other local structures that have can be connected to the same right neighbors. Each ratio is calculated by dividing the concentration of the selected structure by the sum of its concentration and the concentrations of all the found structures. All the results below were obtained by both local models using five-segment simulations, and the same ratio was computed from the naive model for comparison purpose.

We first selected the local structure shown at the top of Fig. 5, which has segment position two from the left-most position. Local structures that can be connected to the same right neighbors are shown in the rest of the figure. The ratio assumption seemed to be satisfied in this case as shown in Fig. 8. x and y-axes of the graph are time and the ratio of specific connection, respectively.

We then selected the local structure shown at the top of Fig. 6, which has segment position three from the left-most position. The rest of the figure and Fig. 9 are similar to previous case. Although all the ratios were increasing almost in the same way, we can find a slight difference between the local models and the naive one. This result exhibits that both local models are defined by an approximate abstraction technique as we explained.

The last example is the local structure shown at the top of Fig. 7, which also has segment position three from the left-most position. In this case, the ratio assumption was not satisfied because there are big differences compared with previous two examples (Fig. 10).

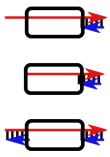

Fig. 5. First example

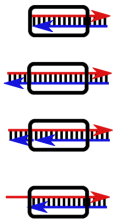

Fig. 6. Second example

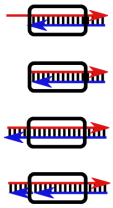

Fig. 7. Third example

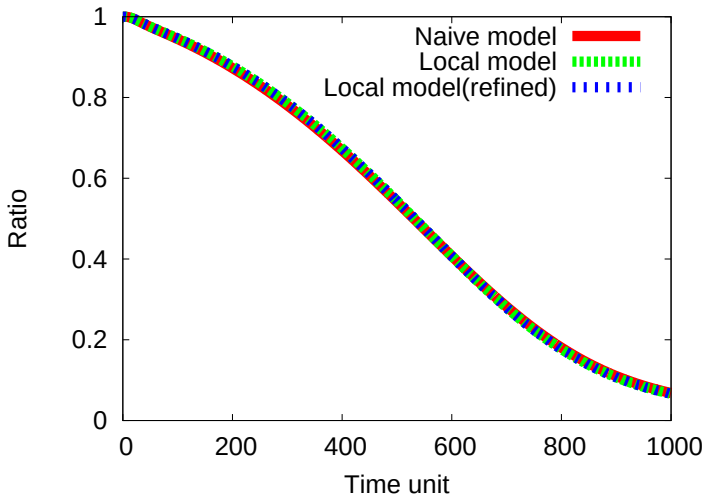

Fig. 8. First ratio

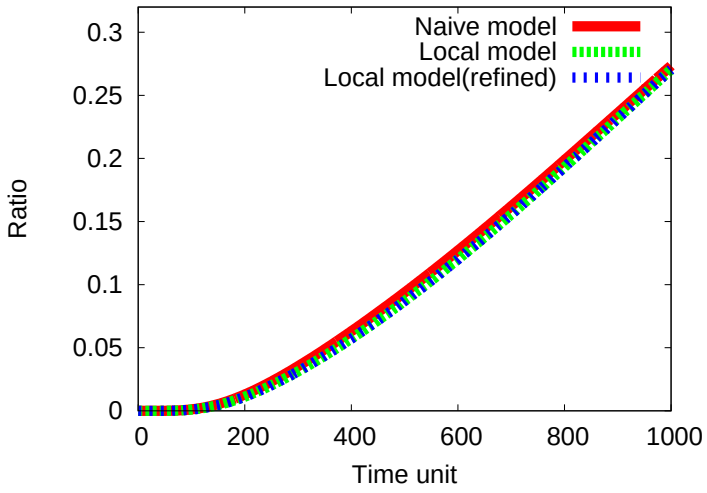

Fig. 9. Second ratio

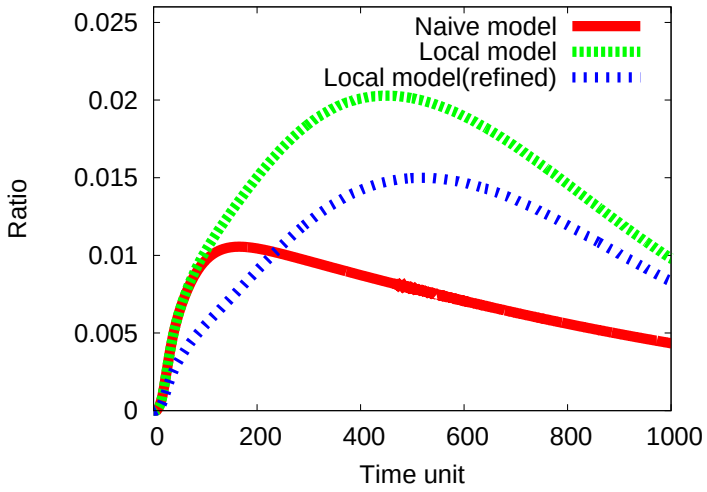

Fig. 10. Third ratio